International Journal of Pure and Applied Mathematics
Volume 112 No. 3 2017, 531-556
ISSN: 1311-8080 (printed version); ISSN: 1314-3395 (on-line version)
url: http://www.ijpam.eu
doi: 10.12732/ijpam.v112i3.7

THE ONSET OF TRAFFIC PHASES IN HIGHWAYS: A TWO VEHICLE-CLASS MACROSCOPIC MODEL

A.R. Méndez[1] §, R.M. Velasco[2]

[1]Departamento de Matemáticas Aplicadas y Sistemas
Universidad Autonoma Metropolitana
Cuajimalpa, MEXICO

[2]Departamento de Física
Universidad Autonoma Metropolitana
Iztapalapa, MEXICO

Abstract: The over-acceleration and adaptation effects in a two vehicle-class mixture of aggressive drivers is studied. A first order model for each vehicle-class is constructed through a kinetic model equation and an iterative procedure. The constructed model is numerically solved with different parameters and under several initial conditions. Numerical results show the onset of the Kerner's phase and suggest that besides the drivers' aggressivity, the most relevant aspect in the adaptation process is the existence of a more numerous vehicle-class.

AMS Subject Classification: 82D05
Key Words: traffic flow model, mathematical modelling, kinetic theory

1. Introduction

The study of traffic flow problems in highways has become a great challenge in the whole world, due to its important impact over the society. The detailed study of traffic flow phenomena has evolved from the pioneer work done by Greenshields, whose studies were centered in the relation between the density

Received: September 30, 2016
Revised: December 25, 2016
Published: February 9, 2017

§Correspondence author

of vehicles and their average speed in a road [1]. Since then, several approaches have come out at different levels of description to understand all complex problems present in traffic flow [2, 3, 4, 5, 6, 7, 8, 9]. Going deeper into the traffic flow modeling, we may mention that it is a common feature, in highway traffic, the presence of free and congested regimes, which depend mainly of the vehicles number per unit length in the road. Also, the congested regime presents what has been identified by Kerner as two phases, the synchronized (S) and the moving jam (J) phases. As a consequence, in Kerner's theory there are three different regimes in the time evolution of traffic. Obviously, the transitions between those regimes constitute a problem to face [10, 11]. We should mention that there are some other alternative descriptions in which the synchronized phase in Kerner's theory is not taken as an independent regime, but it is considered as a congested one only [12, 4, 13]. However, considering the characteristics of the three phases in Kerner's theory, we have tried to recognize them within the scope of a kinetic based macroscopic model. The traffic modeling has currently been done from the individual vehicle description up to their collective behavior and has given rise to observed phenomena in real traffic.

In particular, the kinetic approach starts with a mesoscopic point of view in which the vehicular distribution function plays the fundamental role. Such kind of models starts with Prigogine's work [14], who wrote a kinetic equation, similar to the Boltzmann equation in the kinetic theory of gases, to describe the behavior of the vehicular distribution function. Some years latter the Paveri-Fontana kinetic equation was proposed in an extended phase space, where it is considered the drivers desired speed as an independent variable [15]. The ideas behind such kinetic equations were taken to develop macroscopic models as the proper averages over the distribution function [16, 17, 18, 19, 20, 21, 22]. Kinetic equations in traffic flow, as in any other subject, have mathematical characteristics which make them somewhat complicated. This fact makes their analytical solution a challenge which has not been solved in the literature. As a consequence, a method to obtain a good approximation is necessary. However, the most interesting property of them, is that some averages provide us with macroscopic equations for the relevant collective variables we have chosen to describe the problem. Once the macroscopic model is complete, the numerical solutions can be compared with empirical data taken from real traffic situations.

In this work we will present a macroscopic model for a two-class vehicles system moving unidirectionally. The model is based on the Paveri-Fontana equation (PFE) which introduces a the new variable called desired speed, an average over the desired speed allow us to obtain a kinetic equation in a reduced

phase space. As a consequence of the introduction of the aggressive drivers model [19, 23, 24], we can obtain the distribution function for the homogeneous steady state (equilibrium state) in an analytical way, and this is the basis for an approximate method to go far from such state. As a result, a first order deviation in the average speed gradient is obtained for the distribution function of each class, which is taken to obtain a closure relation. Accordingly to the usual methods in kinetic theory, the averages lead to the balance equations of motion. In our case we will consider the density of each class of vehicles and their corresponding average speeds as relevant variables, so we have a 4-variable model. Then an iterative procedure allows the reduction of variables to just the density of each vehicle class, consequently we will work with a 2-variable model. The numerical solution is obtained for periodic boundary conditions, as well as in the case of an open portion of a highway. Also, we have considered different sets of initial conditions to reproduce some empirical traffic properties. As a result we have obtained that our model give rise to the characteristics of the three phases in Kerner's theory. In particular, the transition $F \to S$ has already been identified through the recognition of the traffic breakdown followed by a fixed front wave on the highway [21].

Section 2 presents the kinetic model starting with the kinetic equation, the solution for homogeneous steady states, the distribution function for local equilibrium states and the modeling for the interaction term. In Section 3 we construct the macroscopic model. Section 4 presents and discusses the numerical results obtained for different initial conditions, where the Kerner's phases appear. Finally, in Section 5 we emphasize the obtained results and compare with real traffic phenomena.

2. Multiclass Traffic Modelling

Some attempts have been made in order to describe multiclass traffic. For example, an early model was presented in 1997 by Daganzo [25] who proposed a phenomenological two class model with the aim to describe kinematic waves in freeways with reserved lanes. This model is a generalization of the Lighthill and Whitham one class model [26] and unfortunately carries out its shortcomings. In 2000 Hoogendoorn and Bovy [27] presented a notable multiclass macroscopic model based on a gas-kinetic equation and a phenomenological closure. Other proposals are presented in [28, 29]. In this manuscript we deal with the construction of a multiclass kinetic based macroscopic model assuming the agressive drivers model presented in [19]. This kind of models centers its

attention in the space-time evolution of the one vehicle distribution function of i-class, $f_i(x, v_i, t)$ where $f_i(x, v_i, t)dxdv_i$ gives us the number of vehicles of the $i-$class in position $(x,\ x + dx)$ with speed $(v_i,\ v_i + dv_i)$ at time t.

Our approach is based on set of coupled Paveri-Fontana-like equations [15] of the type

$$\frac{\partial f_i(v_i)}{\partial t} + v_i \frac{\partial f_i(v_i)}{\partial x} + \frac{\partial}{\partial v_i}\left[\frac{W_i(v_i) - v_i}{\tau_i} f_i(v_i)\right] = \sum_{j=a,b} \mathcal{Q}_{ij}\left(f_i f_j\right) \tag{1}$$

for each class and we restricts our model to a binary one, so $i, j = a, b$. Here, we must mention that we will use the abbreviated notation $f_i(v_i) = f_i(x, v_i, t)$ and $W_i(v_i) = W(x, v_i, t)$ when necessary. The changes in the distribution function due to binary interactions between vehicles is given by

$$\mathcal{Q}_{ij}\left(f_i f_j\right) = (1 - p_i) \int_0^\infty dw f_i(x, v, t) f_j(x, w, t)(w)(w - v), \tag{2}$$

where p_i is the overtaking probability of i vehicles-class. On the other hand, consistently with the ideas of Paveri-Fontana, $W_i(x, v_i, t)$ represents the average of the individual desired speed and must be modeled as a function of the instantaneous speed of drivers (v_i). For the desired speed we consider a model that takes into account aggressiveness of drivers through a parameter which measures how much a driver wishes to increase its actual speed, then we assume

$$W_i(x, v_i, t) = \omega_i v_i, \qquad \omega_i\ >\ 1, \tag{3}$$

where ω_i depends on drivers aggressivity and/or traffic conditions along the highway, (see Figure 1 in reference [23]).

The macroscopic variables describing the dynamical behavior of our system are

$$\rho_i(x, t) = \int_0^\infty f_i(x, v_i, t) dv_i, \qquad \rho(x, t) = \sum_i \rho_i(x, t) \tag{4}$$

$$\rho_i(x, t) V_i(x, t) = \int_0^\infty f_i(x, v_i, t) v_i dv_i \tag{5}$$

$$\rho(x, t) V(x, t) = \sum_{i=a,b} \int_0^\infty v_i f_i(x, v_i, t) dv_i \tag{6}$$

where $\rho_a(x, t),\ \rho_b(x, t)$ are the densities of each class, $\rho(x, t)$ the total density, $V_a(x, t),\ V_b(x, t)$ the corresponding average speeds and $V(x, t)$ the barycentric

speed, all of them being functions of (x,t), and corresponding to the moments of the distribution function. Here we point out that we will omit the (x,t) dependence when necesary. It should be noticed that the integration range in Eqs. (4-6) is not bounded, a usual practice in kinetic theory. It should be noticed that the distribution functions must satisfy proper boundary conditions [23]

$$\lim_{v_i\to 0} f_i(x,v_i,t)=0, \qquad \lim_{v_i\to\infty} f_i(x,v_i,t)=0,$$

both conditions representing the fact that the probability of finding vehicles with $v_i\to 0$ and $v_i\to\infty$ vanishes, otherwise the problem has any sense. Then, if we assume that the probability of overtaking p is the same for all vehicles and introduce the definitions given in Eqs. (4-6) in the interaction term (2) one obtains

$$\begin{aligned}\mathcal{Q}_{aa}+\mathcal{Q}_{ab} &= (1-p)f_a(v_a)\big[\rho_a(V_a(x,t)-v_a)+\rho_b(V_b(x,t)-v_a)\big],\\ \mathcal{Q}_{bb}+\mathcal{Q}_{ba} &= (1-p)f_b(v_b)\big[\rho_b(V_b(x,t)-v_b)+\rho_a(V_a(x,t)-v_b)\big],\end{aligned}$$

where the instantaneous speed as well as position and time dependence is shown.

2.1. The Homogeneous Steady States

First of all, we want to obtain a solution valid for the homogeneous steady states, then we take the equations (1) and (2) and assume that the distribution functions $f_a,\ f_b$ do not depend on position and time, and the model parameters $(\omega_i,\ p,\ \tau_i)$ have constant values. The equations are solved immediately and their solution is given by

$$f_{ie}(v_i)=\frac{\rho_{ie}\alpha_i}{\Gamma(\alpha_i)V_e}\left(\frac{\alpha_i v_i}{V_e}\right)^{\alpha_i-1}\exp\left[-\frac{\alpha_i v_i}{V_e}\right], \tag{7}$$

where the index e is used to allude to the homogeneous steady state, usually known as the equilibrium state, $\Gamma(x)$ is the gamma function and the definitions given in Eqs. (4-6) have been introduced, besides we have defined

$$\alpha_i=\frac{\tau_i(1-p)}{\omega_i-1}\rho_e V_e, \qquad i=a,b \tag{8}$$

as a constant dimensionless quantity which depends on the model parameters $(\tau_i,\ \omega_i,\ p)$ and the characteristics of the homogeneous steady state $(\rho_e,\ V_e)$.

2.2. The Shannon's Information Entropy

The solution we have just found, describes only the homogeneous steady states and to go further it will be considered as a reference to study the dynamics of our problem. To do such a task we need a distribution function $f_i(x, v_i, t)$ consistent with the values of the macroscopic variables we have chosen, in this case $\rho_i(x,t), V_i(x,t)$. The consistency criterion proposed in this paper is provided by the maximization of the Shanon's information entropy defined

$$\mathcal{S}[f\,(x, v_i, t)] = \sum_i \int_0^\infty f_i\,(x, v_i, t) \ln\left(\frac{f_i\,(x, v_i, t)}{f_{ie}}\right) dv_i. \tag{9}$$

Then, the distribution function to be found will be the "best" accordingly with the densities and average speeds considered as relevant variables defined in Eqs. (4-6), this procedure is carried out using the method of Lagrange multipliers, and the result is given by

$$f_i^{(0)}(x, v_i, t) = \frac{\rho_i(x,t)\alpha_i}{\Gamma(\alpha_i)V_i(x,t)}\left(\frac{\alpha_i v_i}{V_i(x,t)}\right)^{\alpha_i - 1} \exp\left[-\frac{\alpha_i v_i}{V_i(x,t)}\right], \tag{10}$$

this local distribution function has the same structure than the one given in Eq. (7), however it now contains the local variables $\rho_i(x,t),\ V_i(x,t)$.

2.3. The Interaction Modeling

In order to consider dissipative effects in our model, we use a very common hypothesis in kinetic theory. Such hypothesis allows one to express the complete solution to Eq. (1) as an infinite expansion in terms of an inhomogeneity parameter which quantifies the deviation from the zero order distribution function due to the gradients present in the system [30]. To first order in this parameter we have

$$f_i(x, v_i, t) = f^{(0)}(x, v_i, t)\big[1 + \phi_i(x, v_i, t)\big], \tag{11}$$

where the function $\phi_i(x, v_i, t)$ represents the deviation from the local approximation $f_i^{(0)}(x, v_i, t)$. It must satisfy the compatibility conditions

$$\rho_i(x,t) = \int_0^\infty f_i(x, v_i, t) dv_i, \tag{12}$$

$$\rho_i(x,t)V_i(x,t) = \int_0^\infty v_i f_i(x, v_i, t) dv_i, \tag{13}$$

which imply that the function $\phi_i(x, v_i, t)$ is restricted by

$$\int_0^\infty \phi_i f_i^{(0)} dv_i = 0, \qquad \int_0^\infty v_i \phi_i f_i^{(0)} dv_i = 0, \quad i = a, b. \tag{14}$$

Now, it is assumed that the interaction term can be written in a similar way as it was done in reference [31] for a mixture of gases

$$\mathcal{Q}_{ii} + \mathcal{Q}_{ij} = f_i^{(0)} \left[-\sigma_i \phi_i(x, v_i, t) + \epsilon_i + \eta_i \left(v_i - V_i(x, t) \right) \right], \tag{15}$$

where σ_i^{-1}, $(i = a, b)$ are parameters which measure a kind of collective relaxation time, they come from a BGK approximation method in the kinetic equation [31, 19] and the quantities ϵ_i, η_i are determined by means of the compatibility conditions, Eqs. (12-13) and are given by

$$\begin{aligned} \epsilon_i(x, t) &= (1 - p)\rho_j(V_j(x, t) - V_i(x, t)), \quad i, j = a, b \\ \eta_i(x, t) &= -(1 - p)\rho(x, t), \quad i, j = a, b. \end{aligned} \tag{16}$$

In order to calculate the function $\phi_i(x, v_i, t)$ we substitute Eq. (15) on the right hand side of the kinetic equations (1) and $f^{(0)}$ on the left [30]. The result is

$$\phi_i \left(x, v_i, t \right) = \frac{1}{\sigma_i} \left[1 + \frac{2 \left(v_i - V_i \right)}{V_i} - \frac{\alpha_i \left(v_i - V_i \right)^2}{V_i^2} \right] \frac{\partial V_i}{\partial x}. \tag{17}$$

The distribution function obtained for each vehicle class is obtained in terms of the local macroscopic variables $\rho_i(x, t), V_i(x, t)$ and the gradient of the average speed. It should be emphasized that these distribution functions satisfy all compatibility equations (12-13), in such a way that we can claim that the relevant variables calculated with the distribution function $f_i(x, v_i, t)$ are the same that the ones specified by the local distribution functions $f_i^{(0)}$, as it should be.

3. The Macroscopic Multiclass Model

The transport equation which describes the evolution of the local variables is obtained when the kinetic equation (1) is multiplied by $\Psi(x, v_i, t)$ and integrated over all the velocity range. If one considers $\Psi(x, v_i, t) = 1$, the result is the evolution equation for the density of each vehicle class

$$\frac{\partial \rho_i}{\partial t} + \frac{\partial \rho_i V_i}{\partial x} = (1 - p)\rho\rho_i(V - V_i), \quad i = a, b \tag{18}$$

we should notice that equations (18) do not correspond to conservation equations, the source of the density of a-class vehicles is the negative of the b-class vehicles. It is only the total density $\rho_a+\rho_b$ the conserved quantity, which means that the total number of vehicles $a+b$ remains constant, in the cases with no entrance or exit ramps.

Similarly, when $\Psi(x, v_i, t) = v_i$ is considered, we obtain the equations of motion

$$\frac{\partial V_i}{\partial t} - \frac{V_i}{\rho_i}\frac{\partial \rho_i V_i}{\partial x} + \frac{1}{\rho_i}\frac{\partial \mathcal{P}_i}{\partial x} - \gamma_i V_i = -(1-p)\rho\theta_i, \quad i = a, b \tag{19}$$

where $\gamma_i = (\omega_i - 1)/\tau_i$ and the traffic pressure and speed variance defined by

$$\mathcal{P}_i(x,t) = \int f_i v_i^2 dv_i, \tag{20}$$

$$\rho_i(x,t)\,\theta_i(x,t) = \int f_i (v_i - V_i(x,t))^2 dv_i, \tag{21}$$

respectively for each vehicle class.

However, balance equations (18-19) constitute a non closed set of equations until the traffic pressure is specified in terms of the relevant variables. If we chose to calculate the traffic pressure and speed variance in (20,21) using the distribution function in (10), the result is $\mathcal{P}_i^{(0)} = \rho_i V_i^2 (\alpha_i + 1)/\alpha_i$ and $\theta_i^{(0)} = V_i^2/\alpha_i$, then the dynamical equations, equivalent to the Euler's equations in fluid dynamics are given by equation (18) which describes the density variations and

$$\frac{\partial V_i}{\partial t} + \left(\frac{\alpha_i + 2}{\alpha_i}\right) V_i \frac{\partial V_i}{\partial x} + \frac{V_i}{\alpha_i \rho_i}\frac{\partial \rho_i}{\partial x} = \frac{V_i}{\gamma_i} - (1-p)\rho\frac{V_i^2}{\alpha_i}, \tag{22}$$

for the average speeds. When equation (11) for $f^{(1)}(x, v_i, t)$ is assumed to calculate the traffic pressure, we get

$$\mathcal{P}_i^{(1)} = \rho_i V_i^2 + \rho_i \theta_i^{(1)} \qquad \text{and} \qquad \rho_i \theta_i^{(1)} = \frac{\rho_i V_i^2}{\alpha_i}\left[1 - \Gamma_i \frac{\partial V_i}{\partial x}\right], \tag{23}$$

where both $\mathcal{P}_i^{(1)}(x,t)$ and $\theta_i^{(1)}(x,t)$ are functions of (x,t) through the density, the average speed and the speed gradient and $\Gamma_i = 2(\alpha_i + 1)/(\sigma_i \alpha_i)$. It is worth mentioning that this result depends on the dimensionless quantity α_i and the parameter introduced in the interaction term σ_i, which is a frequency, and its reciprocal can be interpreted as a collective relaxation time in the distribution function, as can be seen in Eq. (15). So we can rewrite equations

(18-19) in its closed form as

$$\frac{\partial \rho_i}{\partial t} + \frac{\partial \rho_i V_i}{\partial x} = (1-p)\rho_i \rho_j (V_j - V_i), \tag{24}$$

$$\frac{\partial V_i}{\partial t} + V_i \frac{\partial V_i}{\partial x} + \frac{1}{\rho_i}\frac{\partial \rho_i \theta_i^{(1)}}{\partial x} = \frac{V_i}{\gamma_i} - (1-p)\rho \theta_i^{(1)}, \tag{25}$$

for $i, j = a, b,\ j \neq i$, and $\theta_i(x,t)^{(1)}$ given in (23). Equations (24-25) are nonlinear and coupled between themselves. Besides, it is necessary to specify the boundary and initial conditions for all relevant variables, in order to solve them. It is worth noticing that the set of macroscopic equations (24-25) in the homogeneous steady state drives us to $V_{ae} = V_{be} = V_e$, with $\rho_{ae},\ \rho_{be}$ and ρ_e constants, consistent with the conditions imposed to calculate the distribution function describing the equilibrium state. In order to test the model we will use an iterative method to reduce the number of relevant variables [32]. It means that we will take the local solution as a basis and will approximate the deviation from it.

3.1. The Iterative Procedure

Let us assume that the local distribution function $f_i^{(0)}$ drives to the leading contributions in the macroscopic variables, however it is well known that Euler's equations are not good enough to describe a system with non-negligible interactions. As a consequence we want to calculate the corresponding deviations, then we define

$$\hat{V}_i = V_i - V_i^{(0)}, \tag{26}$$

where $V^{(0)}(x,t)$ is the reference speed that we propose as $V_i^{(0)}(x,t) = V_e(\rho_i(x,t))$ inspired in the homogeneous and steady solution of Euler-like equations (18) and (22). Now we introduce Eqs. (23) and (26) in the equation of motion (25) and take up to first order in the speed gradients, to obtain

$$\begin{aligned}
&\frac{\partial \hat{V}_i}{\partial t} + \frac{\partial \hat{V}_i}{\partial x} + \frac{1}{\alpha_i \rho_i}\frac{\partial \rho_i \big(\hat{V}_i^2 + 2\hat{V}_i V_i^{(0)}\big)}{\partial x} + \frac{\partial \big(\hat{V}_i + V_i^{(0)}\big)}{\partial x}\hat{V}_i \\
&-\frac{\Gamma_i}{\alpha_i \rho_i}\frac{\partial}{\partial x}\left(\rho_i \big(\hat{V}_i + V_i^{(0)}\big)^2 \frac{\partial \big(\hat{V}_i + V_i^{(0)}\big)}{\partial x}\right) = \gamma_i \hat{V}_i \\
&-\frac{(1-p)\rho}{\alpha_i}\big(\hat{V}_i^2 + 2\hat{V}_i V_i^{(0)}\big)\left[1 - \Gamma_i \frac{\partial \big(\hat{V}_i + V_i^{(0)}\big)}{\partial x}\right]
\end{aligned} \tag{27}$$

$$+\frac{(1-p)}{\alpha_i}\rho {V_i^{(0)}}^2 \Gamma_i \frac{\partial\left(\hat{V}_i + V_i^{(0)}\right)}{\partial x}.$$

In the left hand side we consider $\hat{V}_i = 0$ and neglect all terms in which second order derivatives appear, then

$$0 = \gamma_i \hat{V}_i - 2\,(1-p)\,\rho \hat{V}_i V_i^{(0)} \frac{1}{\alpha_i} + (1-p)\,\rho {V_i^{(0)}}^2 \left[\frac{\Gamma_i}{\alpha_i}\frac{\partial V_i^{(0)}}{\partial x}\right], \tag{28}$$

which allows us to find the deviation from the zeroth order speed

$$\hat{V}_i = -\frac{\rho {V_i^{(0)}}^2 \Gamma_i}{\left[\rho_e V_e - 2\rho V_i^{(0)}\right]}\frac{\partial V_i^{(0)}}{\partial x}, \tag{29}$$

we recall that the complete speed is $V_i = V_i^{(0)} + \hat{V}_i$. This expression should be introduced in equations (24) in order to get a closed model. Note that the proposed hypothesis $V_i^{(0)} = V_e(\rho_i)$, drive us to have the deviations from the local state $\hat{V}_i$ written in terms of the corresponding density, hence the closure in the macroscopic equations will be given only in terms of densities.

At this point, we want to emphasize that our model contains the free parameters α_i and Γ_i. The parameter Γ_i is a kind of effective relaxation time to the reference distribution function. Besides, α_i has been interpreted before [23] as the inverse of the variance prefactor and is related to the aggressivity parameter (ω_i), in an inversely proportional relation implying that a higher parameter α_i means a lower aggressivity, as shown in Eq. (8).

4. Numerical Results

The obtained model for the densities can now be written in the following dimensionless and conservative form

$$\frac{\partial \mathbf{U}}{\partial t} + \frac{\partial \mathbf{Q}\,(\mathbf{U})}{\partial x} = \mathbf{S}\,(\mathbf{U}) \tag{30}$$

where

$$\mathbf{U} = \begin{pmatrix} \rho_a \\ \rho_b \end{pmatrix}, \mathbf{Q} = \begin{pmatrix} Q_a \\ Q_b \end{pmatrix}, \mathbf{S} = \begin{pmatrix} (1-p)\eta\rho_a\rho_b\,[V_b - V_a] \\ (1-p)\eta\rho_a\rho_b\,[V_a - V_b] \end{pmatrix} \tag{31}$$

with $Q_i = \rho_i \left(V_i^{(0)}(\rho_i) + \hat{V}_i \right)$ for $i = a, b$, $\hat{V}_i$ given in (29) and we have assumed that $V_i^{(0)} = V_e(\rho_i)$ from the fundamental diagram

$$V_e(\rho) = \left[1 + \exp\left(\frac{\rho - 0.25}{0.06} \right) \right]^{-1} - 3.72 \times 10^{-6}, \tag{32}$$

so $V_i^{(0)}$ depends on (x,t) through ρ_i.The dimensionless variables are given in terms of the maximum density ρ_0 and speed V_0 by $\hat{t} = t/\tau$, $\hat{x} = x/V_0\tau$, $\hat{\rho} = \rho/\rho_0$ and $\hat{V} = V/V_0$ and hats have been omitted to clarify notation. In the dimensionless parameter $\eta = \tau\rho_0 V_0$, we have introduced a characteristic relaxation time τ, the maximum speed of the road V_0 and the maximum density ρ_0. In order to solve numerically the system in (31) we choose a road of length L, $N \in \mathbb{N}$ and discretize the space as $h = L/N$ and time by $\Delta t = T/M$ where T is the total simulation time and $M \in \mathbb{N}$ so we have $x_i = ih$, $i = 1, \ldots, N$ and $t_j = j\Delta t$, $j = 1, \ldots, M$. In this sense we use ρ_{ki}^j to denote the approximation $\rho_k(x_i, t_j)$ and

$$\rho_{ki}^0 = \rho_k(x_i, 0), \qquad \rho_{k0}^j = \rho_{k0}^j(0, t_j) = \rho_{kN}^j = \rho_k(x_N, t_j) \tag{33}$$

are the initial and periodic boundary conditions. We apply the Lax-Wendroff iterative procedure [33] with

$$Q_k(U_{ki}^j) = U_{ki}^j V_e(U_{ki}^j) - \frac{\Gamma_k (U_{ai}^j + U_{bi}^j) V_e^2(U_{ki}^j) V_e'(U_{ki}^j)}{[\rho_e V_e - 2(U_{ai}^j + U_{bi}^j) V_e(U_{ki}^j)]} U_{ki}^j \frac{\partial U_{ki}^j}{\partial x} \tag{34}$$

where $k = a, b$ and we have used finite centered differences to approximate the derivative. In the results presented we have considered the following values for the quantities $\Delta x = 0.075$, $\Delta t = 0.375$, $\rho_0 = 140\ veh/km$, $V_0 = 120\ km/h$ and $\tau = 30\ s$.

4.1. Free Flow

In Figure 1 we can see the simulation with the dimensionless parameters $\alpha_a = 120$, $\alpha_b = 100$, $\Gamma_a = 0.012$, $\Gamma_b = 0.06$, for a highway of length $L = 12\ km$, the initial state is given by

$$\begin{aligned} \rho_a(x, 0) &= \rho_e \left[0.45 + 0.05 \sin\left(\frac{2\pi x}{L} \right) \right], \\ \rho_b(x, 0) &= \rho_e \left[0.55 + 0.05 \sin\left(\frac{2\pi x}{L} \right) \right], \end{aligned} \tag{35}$$

where $\rho_e = 0.20$ and we have taken periodic boundary conditions. Notice should be made that the initial perturbation in a-class vehicles goes in phase with b-class. In these cases, both classes of vehicles have almost the same density, and the less numerous a-class (and also the less aggressive) adapts to the more numerous b-class, contributing so to rise the b-class density. A traveling cluster propagates upstream and finally, for long times, the cluster dissolves itself. The long time behavior on this situation ($L = 12\ km$) is shown at the bottom of Figure 1, where a kind of steady-state is reached.

A similar simulation was made for a highway of length $24km$ and the results are qualitatively similar so we conclude that the length of the road does not play a relevant role, so henceforth we will perform all the simulations for $L = 12\ km$ only.

Figure 2 shows the simulation using parameters given before, in a highway of length $L = 12\ km$, and an initial state specified as follows

$$\begin{aligned} \rho_a(x,0) &= \rho_e \left[0.2 + 0.05 \sin\left(\frac{2\pi x}{L}\right)\right] \\ \rho_b(x,0) &= \rho_e \left[0.8 + 0.05 \sin\left(\frac{2\pi x}{L}\right)\right], \end{aligned} \tag{36}$$

also periodic boundary conditions are taken. Unlike the last cases, now we have very different initial densities for each vehicle-class and the behavior is similar. The more scarce and less aggressive a-class adapts itself to increase the b-class density. Also a traveling wave propagating upstream is developed. The long time behavior for this case is shown at the bottom of Figure 2 where we observe that a steady-state is reached. Figure 1 and Figure 2 must be compared to note that the proportions between different vehicles classes is essential to determine the adaptation time, in Figure 1 where both classes are almost in the same proportions the adaptation occurs in a longer time that in Figure 2 where adaptation happens in a very sudden way. Now we interchange the role in the aggressivity parameter, the more numerous class, the a-class, is the less aggressive one, and the less numerous b-class is the more aggressive. (Figure 3) shows the simulation for this case with the initial state

$$\begin{aligned} \rho_a(x,0) &= \rho_e \left[0.8 + 0.05 \sin\left(\frac{2\pi x}{L}\right)\right] \\ \rho_b(x,0) &= \rho_e \left[0.2 + 0.05 \sin\left(\frac{2\pi x}{L}\right)\right]. \end{aligned} \tag{37}$$

The results in Figure 2 and Figure 3 show that the relevant aspect in the

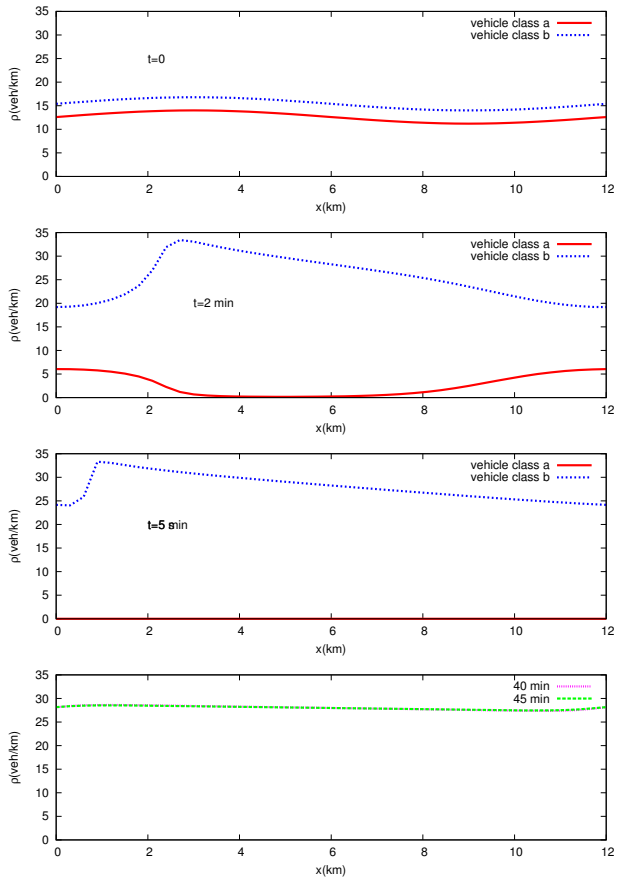

Figure 1: The sequence of the density profile for different times ($L = 12\ km$). We have used parameters given before, the initial state in (35) and periodic boundary conditions. At the bottom the long time behavior of the survival vehicle class.

dynamics is not aggressiveness but the relative density between classes, the most numerous being the leading one. It must be emphasized that although the aggressivity parameter does not determine which one of the classes adapts, the differentiation between classes allows us to have an adaptation effect. The bottom graph in Figure 3 shows the long time behavior for the survival vehicle class for this situation.

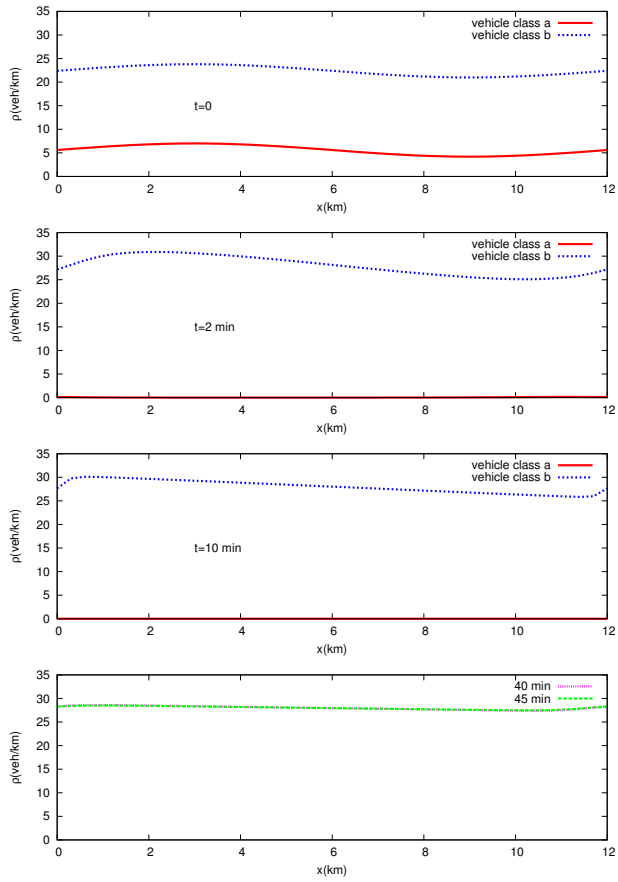

Figure 2: The sequence of the density profile for different times ($L = 12\ km$). We have used the initial state in (36) and periodic boundary conditions. At the bottom, the long time behavior of the survival vehicle class.

4.2. Free-Synchronized Flow Transition

The $F \to S$ flow transition is observed in our model without a bottleneck in very special conditions, the detailed analysis can be seen in [21] and we include this subsection just for the sake of completeness. In fact, this transition is observed when the initial conditions in the densities are out of phase, this means that an over-acceleration effect in the most aggressive class of drivers is present together with the mentioned adaptation behavior.

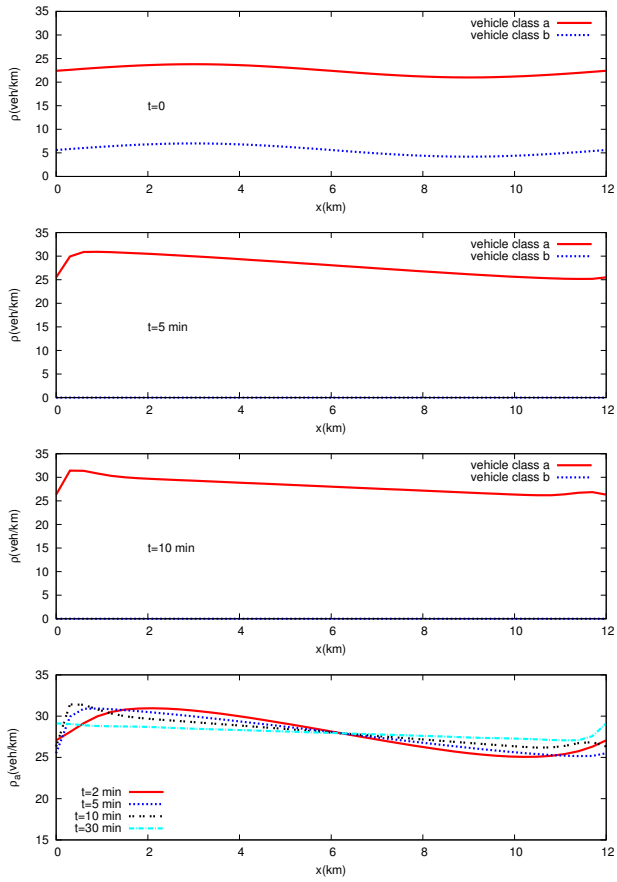

Figure 3: The initial density profile and a sequence for different times for the survival class ($L = 12\ km$), with the initial state given in (37) and periodic boundary conditions. The long time behavior corresponds to a practically homogeneous situation for the survival class.

In order to give a complete panorama in Figure 4 it is shown the out of phase initial condition

$$\begin{aligned} \rho_a(x,0) &= \rho_e\left[0.85 + 0.1\sin\left(\frac{2\pi x}{L}\right)\right] \\ \rho_b(x,0) &= \rho_e\left[0.15 + 0.1\sin\left(\frac{2\pi x}{L} + \frac{\pi}{2}\right)\right], \end{aligned} \tag{38}$$

at the top, as well as a permanent cluster which appears around the kilometer 11.

In Figure 5 it is possible to appreciate the velocity drop of the survival class after approximately 5 minutes of simulation and around kilometer 11. Also, the companion density profile has a maximum produced suddenly at the same time.

It should be noticed that the results in Figure 4-Figure 5 present the characteristics of the presence of the synchronized phase flow, according to the Kerner's classification. First, a fixed cluster in a highway position and, the traffic breakdown with the values of speed showing a sudden and strong change at a certain point in the highway. This behavior has been produced from an over-acceleration effect in the $b-$class followed by an adaptation to the more numerous $a-$class of drivers. The over-acceleration was produced by an out of phase condition in the perturbation together with the aggressivity of drivers. Should be emphasized that the perturbation produced by the presence of the two classes has its main effects after the transient situation. Such effects are due to the coupling between classes. In this sense, the over acceleration and adaptation effects produce the dynamics. After the perturbation and raising of the traffic phases the system is not perturbed any more and tend to reach an steady state.

4.3. The $S \rightarrow J$ Transition

To go further with the results in this model, we will consider a set of initial conditions which allow the presence of the synchronized phase followed by the transition to a congested phase

$$\rho_a(x,0) = 0.55\rho_e\Big[1+\delta\rho\Big(\cosh^2\Big(\frac{x-6}{0.5}\Big)-\cosh^2\Big(\frac{x-7}{0.5}\Big)\Big)\Big],$$
$$\rho_b(x,0) = 0.45\rho_e\Big[1+\delta\rho\Big(\cosh^2\Big(\frac{x-6}{0.5}\Big)-\cosh^2\Big(\frac{x-7}{0.5}\Big)\Big)\Big]. \qquad (39)$$

Now we take a highway with $L = 12\ km$, $\rho_e = 0.22$, $\delta\rho = 0.1$, and the parameters to characterize the drivers classes are $\alpha_a = 120$, $\alpha_b = 100$, $\Gamma_a = 0.0001$ and lastly $\Gamma_b = 0.0005$. The difference between the initial densities is small. The dynamics shown under these conditions develops a high density moving jam traveling upstream, however it also appears the synchronized phase with a smaller density. The density color map in Figure 6 (at the right) shows both phases, the yellow profile shows a moving jam and the blue profile with a variable speed front represents the synchronized phase. Besides, both profiles join together at certain point in the highway and the region around this point represents the transition $S \rightarrow J$. Figure 6 (at the right) shows the color map

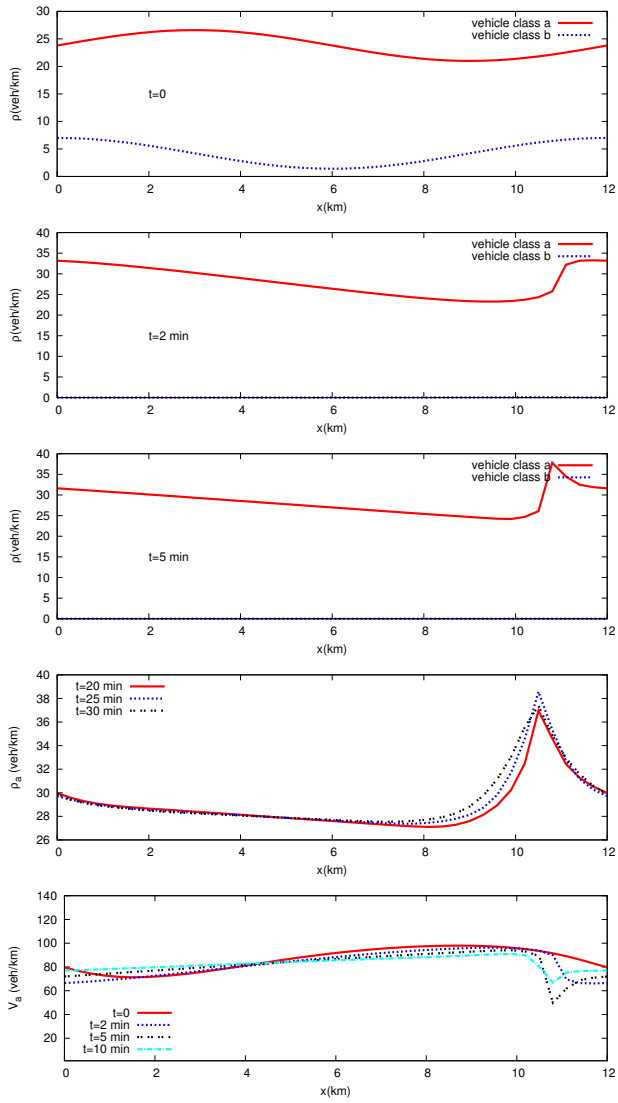

Figure 4: The sequence of the density profile for different times ($L = 12\ km$). We have used the same parameters as in Figure 1, initial state in (38) and periodic boundary conditions. The last one corresponds to the speed profile.

for the survival density and the transition is seen around the fourth kilometer and $t \sim 18\ min$.

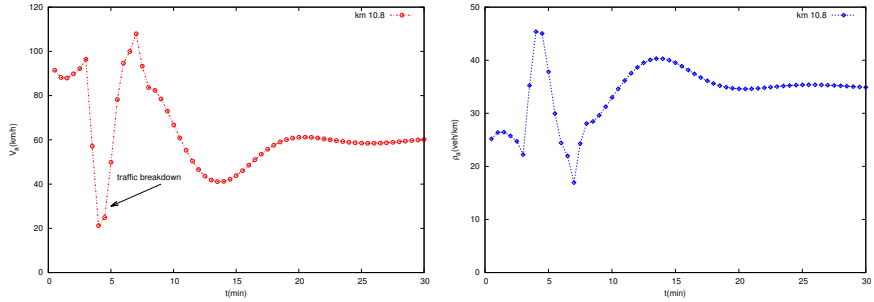

Figure 5: Speed and density profiles at kilometer 10.8. Notice the traffic breakdown around minute 5.

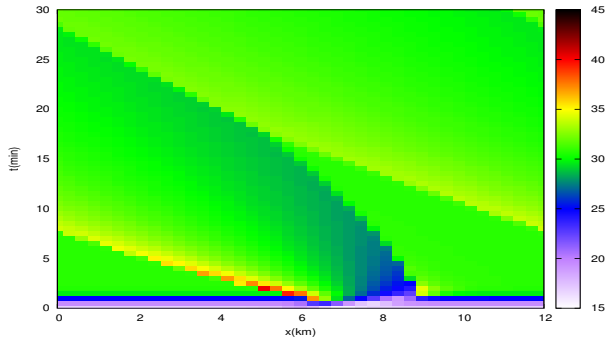

Figure 6: The $S \rightarrow J$ transition in a color code map for the density of the survival class.

The traffic breakdown going with the synchronized phase is shown in Figure 7, at the top, where the average speed of the survival class changes in an abrupt way when we observe the profile at position $x = 5.7\ km,\ t \approx 2.5\ min$ and at position $x = 8.7\ km,\ t \approx 1.5\ min$. The corresponding flow rates for both situations is shown in (Figure 7) and it is clear that flow rate around $x = 8.7\ km$ does not drop abruptly while in $x = 5.7\ km$ it does. After 18 min the synchronized flow reaches the moving jam and they continue traveling upstream with approximately the same velocity and flow rate.

4.4. Traveling Waves

In order to show the formation of traveling waves we have considered a higher density to start the simulations $\rho_e = 0.32$ with $\delta\rho = 0.05$ and the initial condi-

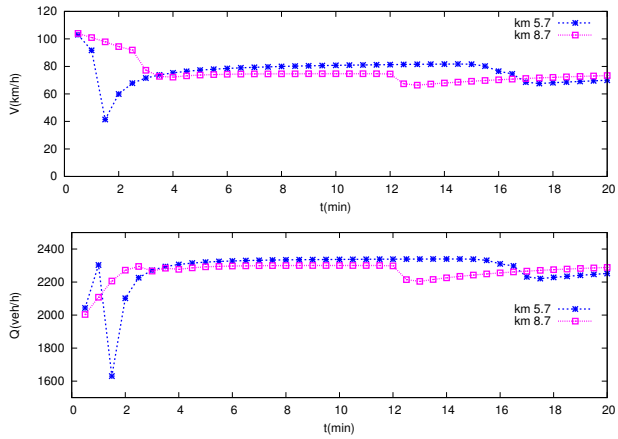

Figure 7: Speed and flow profiles of the survival vehicle class at $x = 5.7\ km$ and $x = 8.7\ km$. It is shown that there is a traffic breakdown, followed with smooth changes in an advanced position.

tions given by

$$\rho_a(x,0) = 0.8\rho_e\Big[1+\delta\rho\Big(\cosh^2\Big(\frac{x-6}{0.5}\Big) - \cosh^2\Big(\frac{x-7}{0.5}\Big)\Big)\Big],$$
$$\rho_b(x,0) = 0.2\rho_e\Big[1+\delta\rho\Big(\cosh^2\Big(\frac{x-6}{0.5}\Big) - \cosh^2\Big(\frac{x-7}{0.5}\Big)\Big)\Big]. \tag{40}$$

(Figure 8) shows the survival density in a color code map for periodic boundary conditions. It is seen in a clear way that there exists a moving wave traveling upstream with constant speed. In (Figure 9), the density profile as well as the speed profile are shown for different times where we see the moving wave traveling upstream.

4.5. Open Boundaries

Until now, we have considered that the total density is conserved, this is clear when we observe the source term in equation (31). From now on, we will modify the source term in (31) for the a-class by a factor 0.25 and the one for the b-class by a factor 0.50. We have not periodicity anymore but in the left hand side of the road a flow rate corresponding with a influx density 0.7 ρ_e is maintained and in the right hand side vehicles can leave the road freely. In figure 10, we have considered $\alpha_a = 120$ $\alpha_b = 100$, $\Gamma_a = 0.012$ and $\Gamma_b = 0.06$ in a highway

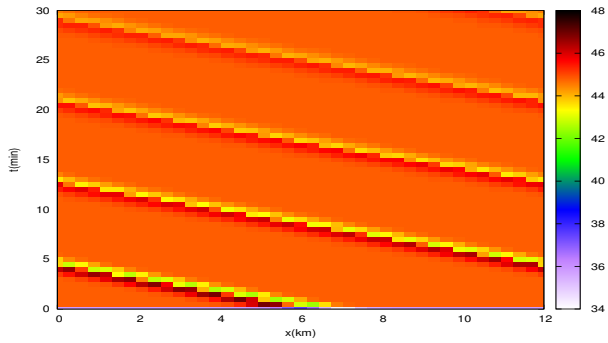

Figure 8: The traveling wave moving upstream with constant speed, $\rho_e = 0.32$.

with $L = 24\ km$ and the initial condition with $\rho_e = 0.20$

$$\rho_a(x,0) = \rho_e\left[0.7 + 0.05\sin\left(\frac{2\pi x}{L}\right)\right]$$
$$\rho_b(x,0) = \rho_e\left[0.3 + 0.05\sin\left(\frac{2\pi x}{L}\right)\right]. \tag{41}$$

In this case, due to the lost of conservation and the influx of vehicles, a low density wave traveling downstream is formed. Again the less numerous b-class adapts to traffic conditions imposed by the more numerous a-class. At the bottom of (Figure 10) we see a kind of steady-state is reached due to the influx in one side of the road. However the free flow traveling wave leaves the right hand side of the highway.

If we interchange the aggressivity values between the drivers classes, the results are very similar, the more numerous vehicle class survives while the other adapts and a low density wave propagates downstream on the highway, a situation which becomes possible because vehicles can leave the road freely. When the simulation begins with a larger density (around 30% of the total occupation) also a high density wave is developed, however it travels upstream as shown in (Figure 11). Again we observe adaptation from the less numerous class to the more numerous one, this adaptation behavior occurs into the first kilometer of the highway. The open boundaries allow traveling waves going downstream or upstream according to the total density of vehicles in the highway, though at long times, a steady state is reached due to the influx and free leaving at right and left extremes.

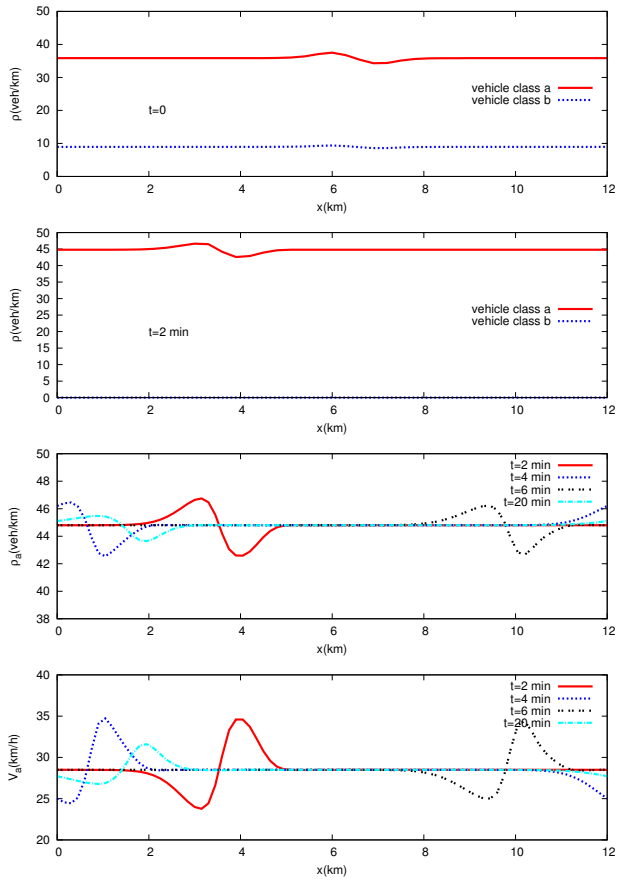

Figure 9: From top to bottom: the initial density profile, density profile at $t = 2\ min$, density and speed profiles of the survival class at several times.

5. Concluding Remarks

We state a set of kinetic equations to describe a system for two-classes of drivers/vehicles with different aggressivity parameter. Through the methods in kinetic theory it is possible to get a macroscopic model where the relevant variables are the densities of vehicle classes. The model is constructed taking as a starting point the reduced Paveri-Fontana kinetic equation and the standard methodology in kinetic theory. As a result we have found a very complex set of equations, so we assumed an iterative procedure, akin to the Maxwell's

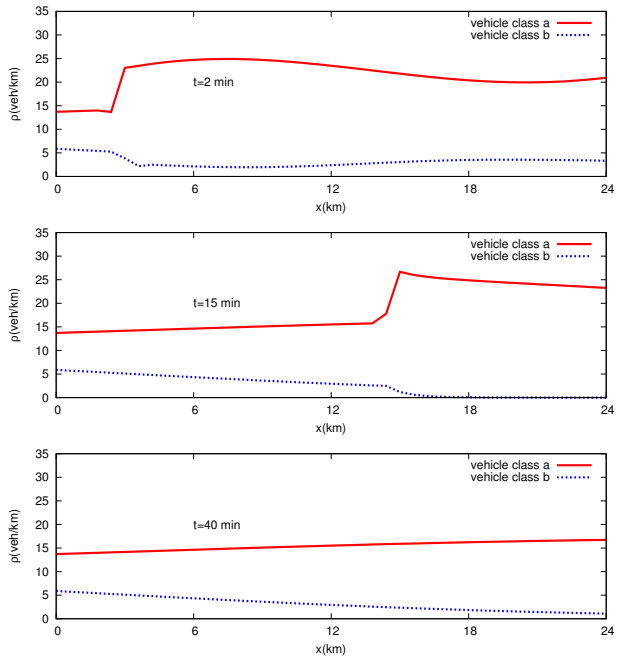

Figure 10: For $L = 24\ km$, the sequence of the density profile at different times. The same parameters as in figure (1) have been used, initial conditions in (41) and a constant influx in the left hand side of the highway. A low density wave appears traveling downstream.

one, in order to have a simpler hydrodynamic description for each one of the vehicle classes. The numerical simulations of our results are computed for different situations in order to test our model. We have observed, that changing the length of the road has not relevant influence in the results, the upstream traveling perturbation developed within the longer road is just slightly flatter than the one in the shorter. The numerical solution in (Figures 2 and 3) show that in order to have an adaptation to the more numerous vehicle class at least two vehicle-classes should exist, but we observe that it is not the aggressivity parameter the relevant feature in this adaptation behavior. In fact, the less numerous vehicle-class, no matter its aggressivity, always adapts to the more numerous one. It means that the less numerous class disappears after the transient, which has produced a perturbation in the whole system dynamics. It is during the transient, where the over-acceleration and adaptation effects take place.

More important than the above observations is the fact that the model is able

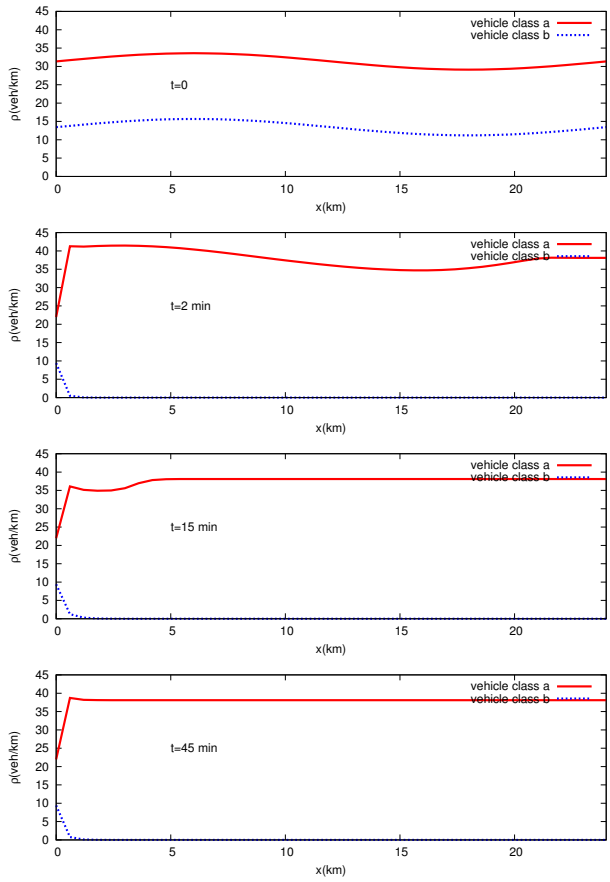

Figure 11: Sequence of density profiles at different times for $L = 24\ km$. The initial conditions given in Eqs. (41) and a constant influx in the left hand side of the highway. A low density wave appears traveling downstream.

to give rise to the characteristic behavior of the three traffic phases as described by the Kerner's theory. In all the cases studied, an initial state is slightly perturbed, as it can be observed the initial perturbation leads to the formation of the phases, this perturbation relaxes after a transient time, because over time all vehicles on the less numerous class transforms into the leading vehicle-class, *i.e.*, one of the densities goes to zero. Under this condition, the right hand side of equation (31) is zero. Therefore, for long times, a steady state is reached. Now, the free phase (F) is established at low density under a small pertur-

bation, we observe that after a transitory, the system reaches a steady state situation as expected. Second, there are certain initial conditions which favor an over-acceleration effect in the more aggressive but less numerous class of vehicles. This fact together with the adaptation behavior noticed above, causes the apparition of the synchronized phase in free flow. The transition between the free and synchronized phases arises at the traffic breakdown and, the phase S remains fixed even without a physical bottleneck, as a consequence of the periodic boundary conditions imposed on the dynamics (see also [21]). Third, the synchronized and wide moving jam J phases may be present simultaneously as shown in 6. Eventually it would happen the transition $S \rightarrow J$ under periodic boundary conditions. For bigger equilibrium density we can find a cluster traveling upstream with constant speed. Lastly, the open boundaries problem may produce a traveling cluster going upstream or downstream according to the influx flow rate. It should be emphasized that all these results have been produced with the same model, just by changing the initial equilibrium density, the parameter values in the model and, the initial conditions.

Acknowledgements

The authors acknowledge support from CONACyT through grant number 251273.

References

[1] B. D. Greenshields, A study of traffic capacity, In *Proceedings of the High-way Research Board*, **14** (1935), 448-477.

[2] B. S. Kerner, *The Physics of Traffic*, Understanding Complex Systems, Springer, Heidelberg (2004), **doi:** 10.1007/978-3-540-40986-1.

[3] B. S. Kerner, *Introduction to Modern Traffic Flow Theory and Control*, Springer-Verlag, Berlin (2009), **doi:** 10.1007/978-3-642-02605-8.

[4] M. Treiber and A. Kesting, *Traffic Flow Dynamics*, Springer-Verlag (2013).

[5] D. Helbing, Traffic and related self-driven many-particle systems, *Rev. Mod. Phys.*, **73**, No. 4 (2001),1067-1141, **doi:** 10.1007/978-3-642-32460-4.

[6] D. Chowdhury and A. Schadsneider, Simulation of vehicular traffic: A statistical physics perspective, *Comput. Sci. Eng.*, **2**, No. 5 (2000), 80-87, **doi:** 10.1109/5992.877404.

[7] S. Maerivoet and B. De Moor, Cellular automata models of road traffic, *Phys. Rep.*, **419**, No. 1 (2005), 1-64, **doi:** 10.1016/j.physrep.2005.08.005.

[8] R. Mahnke, J. Kaupuzs and I. Lubashevsky, Probabilistic description of traffic flow, *Phys. Rep.*, **408**, No. 1-2 (2005), 1-130, **doi:** 10.1016/j.physrep.2004.12.001.

[9] B. S. Kerner, Criticism of generally accepted fundamentals and method-ologies of traffic and transportation theory: A brief review, *Physica A*, **392**, No. 21 (2013), 5261-5282, **doi:** 10.1016/j.physa.2013.06.004.

[10] B. S. Kerner, S. L. Klenov and A. Hiller, Criterion for phases in singe vehicle data and empirical test of a microscopic three-phase traffic theory, *J. Phys. A: Math. Gen.*, **39**, No. 9 (2006), 2001-2020, **doi:** 10.1088/0305-4470/39/9/002.

[11] B. S. Kerner, S. L. Klenov and P. Konhauser, Asymptotic theory of traffic jams, *Phys, Rev. E*, **56**, No.4 (1997), 4200-4216, **doi:** 10.1103/PhysRevE.56.4200.

[12] M. Treiber, A. Kesting and D. Helbing, Three-phase traffic theory and two-phase models with a fundamental diagram in the light of empirical stylized facts, *Transp. Res. B*, **44**, No. 8-9 (2010), 983-1000, **doi:** 10.1016/j.trb.2010.03.004.

[13] M. Schonhof and D. Helbing, Criticism of three-phase traffic theory, *Transp. Res. Part B*, **43**, No. 7 (2009), 784-797, **doi:** 10.1016/j.trb.2009.02.004.

[14] I. Prigogine and R. Herman, *Kinetic Theory of Vehicular Traffic*, Elsevier, New York-London-Amsterdam (1971).

[15] S. L. Paveri-Fontana, On boltzmann-like treatments for traffic flow: A critical review of the basic model and an alternative proposal for dilute traffic analysis, *Transp. Res.*, **9** (1975), 225-235, **doi:** 10.1016/0041-1647(75)90063-5.

[16] C. Wagner, C. Hoffmann, R. Sollacher, J. Wagenhuber and B. Schurmann, Second-order continuum traffic flow model, *Phys. Rev. E*, **54**, No. 5 (1996), 5073-5085, **doi:** 10.1103/PhysRevE.54.5073.

[17] D. Helbing, Improved fluid-dynamic model for vehicular traffic, *Phys. Rev. E*, **51**, No. 4 (1995), 3164-3169, **doi:** 10.1103/PhysRevE.51.3164.

[18] S. P. Hoogendoorn and P. H. L. Bovy, Generic gas-kinetic traffic systems modeling with applications to vehicular traffic flow, *Transp. Res. Part B*, **35** No. 4 (2001), 317-336, **doi:** 10.1016/S0191-2615(99)00053-3.

[19] R. M. Velasco and W. Marques Jr., Navier-stokes-like equations for traffic flow, *Phys. Rev. E*, **72** No. 4 (2005), 046102, **doi:** 10.1103/PhysRevE.72.046102.

[20] A. Bellouquid, E. De Angelis and L. Fermo. Towards the modeling of vehicular traffic as a complex system: A kinetic theory approach, *Math. Models Methods Appl. Sci.*, **22**, No. Supp 01 (2012), 1140003, **doi:** 10.1142/S0218202511400033.

[21] A. R. Méndez and R. M. Velasco, Kerners free-synchronized phase transi-tion in a macroscopic traffic flow model with two class of drivers, *J. Phys. A: Math. Theor.*, **46**, No. 46 (2013), 1-9, **doi:** 10.1088/1751-8113/46/46/462001.

[22] L. Fermo and A. Tosin, A fully-discrete-state kinetic theory approach to modeling vehicular traffic, *SIAM J. Appl. Math.*, **73** No. 4 (2013), 1533-1556, **doi:** 10.1137/120897110.

[23] A. R. Méndez and R. M. Velasco, An alternative model in traffic flow equations, *Transp. Res. Part B*, **42** (2008), 782-797, **doi:** 10.1016/j.trb.2008.01.003.

[24] W. Marques Jr. and A. R. Méndez, On the kinetic theory of vehicular traffic flow: Chapman-Enskog expansion versus Grads moment method, *Physica A*, **392** No. 16 (2013), 3430-3440, **doi:** 10.1016/j.physa.2013.03.052.

[25] C. F. Daganzo, A continuum theory of traffic dynamics for freeways with special lanes, *Trasnp. Res. B*, **31**, No. 2 (1997), 83-102, **doi:** 10.1016/S0191-2615(96)00017-3.

[26] M. J. Lighthill and G. B. Whitham, On kinematic waves. ii. a theory of traffic flow on long crowded roads, *Proc. Roy. Soc. London, Series A, Math, Phys. Sci.*, **229** No. 1178 (1955), 317-345, **doi:** 10.1098/rspa.1955.0089.

[27] S. P. Hoogendoorn and P. H. L. Bovy, Continuum modeling of multiclass traffic flow, *Transp. Res. Part B*, **34**, No. 2 (2000), 123-146, **doi:** 10.1016/S0191-2615(99)00017-X.

[28] S. P. Hoogendoorn and P. H. L. Bovy, Platton-based multiclass modeling of multilane traffic flow, *Networks and Spatial Economics*, **1**, No.1-2 (2001), 137-166, **doi:** 10.1023/A:1011533228599.

[29] S. Looghe and L. H. Immers, Multiclass kinematic wave theory of traffic flow, *Transp. Res. Part B*, **42**, No. 6 (2008), 523-541, **doi:** 10.1016/j.trb.2007.11.001.

[30] S. Chapman and T. G. Cowling, *The Mathematical Theory of Non-Uniform Gases*, Cambridge Mathematical Library, United Kingdom (1970).

[31] A. S. Fernandes and W. Marques Jr., Sound propagation in binary gas mixtures from a kinetic model of the boltzmann equation, *Physica A*, **332** (2004), 29-46, **doi:** 10.1016/j.physa.2003.10.028.

[32] G. Medeiros-Kremer, *An Introduction to the Boltzmann Equation and Transport Processes in Gases*, Springer-Verlag Berlin Heidelberg (2010), **doi:** 10.1007/978-3-642-11696-4.

[33] D. Helbing and M. Treiber, Numerical simulation of macroscopic traffic equations, *Comput. Sci. Eng.*, **1**, No. 5 (1999), 89-99, **doi:** 10.1109/5992.790593.